Journal of Applied Crystallography

ISSN 0021-8898

Received 0 XXXXXXX 0000
Accepted 0 XXXXXXX 0000
Online 0 XXXXXXX 0000

Extracting the pair distribution function (PDF) from white beam x-ray total scattering data

Alan K. Soper* and Emma R. Barney

ISIS Facility, STFC Rutherford Appleton Laboratory, Harwell Science Innovation Campus, Didcot, Oxon, OX11 0QX England. Correspondence e-mail: alan.soper@stfc.ac.uk

A general method is described for reducing white beam x-ray total scattering raw data to differential scattering cross section (DCS) and pair distribution function (PDF). The method incorporates corrections for x-ray fluorescence, bremsstrahlung radiation, polarization, attenuation, multiple scattering, and sample container scattering, and invokes the Krogh-Moe and Norman method to put the data on an absolute scale. An accurate method to convert the differential scattering cross section to pair distribution function is also described, and a rigorous and revised Lorch function is proposed for removing the effects of Fourier truncation oscillations. The method can be equally applied to synchrotron x-ray data, where the data analysis can be simpler than at a laboratory source.

1. Introduction - total scattering diffraction measurements

In recent years there has been much interest in developing alternative tools for examining the structure of crystalline materials. A traditional crystal structure refinement involves analysis of the Bragg peaks in a diffraction pattern, and this gives the average, long-time, atomic structure. However, as has been explained elsewhere, (Billinge & Thorpe, 1998; Egami & Billinge, 2003; Tucker *et al.*, 2007), total scattering measurements explore the local, instantaneous atomic structure of a material, glass or liquid, independently from the average unit cell structure that may be present. This local *non-crystalline* order gives rise to weak or very weak diffuse, i.e. non-Bragg, scattering that needs to be measured to good accuracy if it is to give a reliable representation of the local order in a material.

The local order in a material is normally represented by the pair distribution function (PDF), $g(r)$, (Egami & Billinge, 2003), variously called the radial distribution function (RDF) or pair correlation function (PCF), which describes the variation of density as a function of radial distance from any atom in the material. This function is not measured directly by the scattering experiment, which instead measures a Fourier transform of the PDF, the so-called structure function or structure factor, $F(Q)$, where Q is the wave vector change in the scattering experiment. This has to be Fourier transformed back to real (r-) space to obtain the PDF. Hence, from the properties of Fourier transforms, the resolution of peaks in the PDF is directly related to the largest value of Q in the diffraction experiment, $Q_{\rm max}$, which is proportional to the maximum scattering angle, and inversely proportional to radiation wavelength. In order to get to the largest possible $Q_{\rm max}$, and so achieve maximum resolution in the PDF, total scattering experiments tend to use the shortest radiation wavelength practicable, typically $\lessapprox 0.5$ Å. Such short radiation wavelengths are routinely available at reactor or pulsed neutron sources, such as Institut Laue Langevin, Grenoble, France, or ISIS, UK, and at synchrotron x-ray sources, but are less common for laboratory x-ray sources.

Recently in collaboration with the PANalytical company we have specified and purchased an Ag-anode x-ray diffractometer (XRD) which produces a mean K_α radiation wavelength of 0.5609Å, plus K_β and the standard bremsstrahlung radiation. With the maximum scattering angle near 156°, this gives a maximum Q of 21.9Å^{-1}. The diffractometer is designed to enable users of the the ISIS neutron facility to obtain complementary x-ray data for the materials investigated with neutrons. This is because x-ray form factors are quite different in amplitude and variation across the Periodic Table compared to neutron scattering amplitudes. Currently there is no suitable x-ray monochromator for this device, so the K_β radiation is removed using a Rh filter. Nonetheless there is still significant off-energy bremsstrahlung radiation, which because of the range of wavelengths present, has the effect of adding a blurred version of the diffraction profile to the scattering data. In addition, for those elements with absorption edges in the energy range of the incident spectrum, there is the complication of off-energy fluorescent radiation being generated in the material.

In order to rapidly obtain the most reliable data from this machine, a new data analysis program called GudrunX has been developed. Of course this is not by any means the first suite of programs to analyse x-ray data of the kind described above - see for example (Petkov, 1989; Jeong *et al.*, 2001) - but it is the ability to deal simultaneously with bremsstrahlung radiation and fluorescence radiation that distinguishes GudrunX from previous x-ray data analysis programs. Here the underlying formalism behind total scattering analysis is first described in some detail because some aspects of this formalism often go unstated in standard descriptions. This is followed by an outline of how the new program works. In addition the process of reliably calculating the Fourier transform of the structure function is discussed, and a revised version of the Lorch modification function is proposed.

2. Overview of scattering theory

IUCr macros version 2.1.4: 2010/12/07

2.1. The scattering amplitude of a distribution of atoms

If the position of atom i is given by $\mathbf{R}_i$ then the local number density at displacement $\mathbf{r}$ can be expressed as

$$n(\mathbf{r}) = \sum_i \delta(\mathbf{r} - \mathbf{R}_i), \tag{1}$$

where $\delta(\mathbf{r})$ is the Dirac delta-function.

For the radiation scattering experiment, if the atoms behave as point particles this number density will be replaced by a scattering length density,

$$A(\mathbf{r}) = \sum_i b_i \delta(\mathbf{r} - \mathbf{R}_i) \tag{2}$$

where b_i is the scattering length of atom i. Of course x-rays are scattered by the electron density distribution around each atom so the sum over atom positions in (2) becomes a sum over electron positions. Assuming the electron density around each atom is independent of the atom's position (an assumption which is not necessarily valid in every case), then the electron density becomes a convolution of the number density function given by (1) and the independent atom electron density function, $f^{(\mathrm{IA})}(\mathbf{r})$:

$$\begin{aligned} A_x(\mathbf{r}) &= r_e \sum_i \int f_i^{(\mathrm{IA})}(\mathbf{r}')\delta((\mathbf{r} - \mathbf{r}') - \mathbf{R}_i)d\mathbf{r}' \\ &= r_e \sum_i f_i^{(\mathrm{IA})}(|\mathbf{r} - \mathbf{R}_i|) \end{aligned} \tag{3}$$

where r_e is the Thomson scattering length of the electron. Normally the factor r_e is ignored, so that x-ray scattering amplitudes are expressed in (dimensionless) units of electrons. The same convention will be adopted here.

The x-ray is scattered by the whole array of atoms, so the scattered amplitude at some scattering angle 2θ and x-ray wavelength λ is given by

$$\begin{aligned} A_x(\mathbf{Q}) &= \int A_x(\mathbf{r}) \exp(i\mathbf{Q}\cdot\mathbf{r})d\mathbf{r} \\ &= \sum_j f_j^{(\mathrm{IA})}(Q) \exp(i\mathbf{Q}\cdot\mathbf{R}_j) \end{aligned} \tag{4}$$

Assuming the scattering event involves negligible change in the energy of the incident radiation then $Q = \frac{4\pi \sin\theta}{\lambda}$.

The scattering experiment measures the scattered *intensity* proportional to $|A(\mathbf{Q})|^2$, which (including the unwritten factor of r_e), has the units of cross sectional area, so the total structure function or structure factor is represented as the scattering cross section of the material per atom:

$$\begin{aligned} F(\mathbf{Q}) &= \frac{1}{N}|A(\mathbf{Q})|^2 \\ &= \frac{1}{N}\sum_{jk} f_j^{(\mathrm{IA})}(Q) f_k^{(\mathrm{IA})}(Q) \exp[i\mathbf{Q}\cdot(\mathbf{R}_j - \mathbf{R}_k)], \end{aligned} \tag{5}$$

N being the number of atoms.

Note that the sum in (5) can be divided into two parts, namely terms for which $j = k$, the so-called "self" terms, and terms for which $j \neq k$, the "distinct" or "interference" terms. The self terms will carry no information on the relative distribution of atoms because the exponential term in (5) will be exactly unity for these terms, while the remaining terms are in effect measuring the distribution of distinct atoms as a function of displacement from an atom at the origin.

2.2. Relationship with the pair distribution function

The structure of any material is defined via the autocorrelation of the single particle density function, (1):

$$G(\mathbf{r}) = \frac{1}{N}\int d\mathbf{r} n(\mathbf{r}')n(\mathbf{r}'+\mathbf{r}) = \frac{1}{N}\sum_{jk}\delta(\mathbf{r} + \mathbf{R}_j - \mathbf{R}_k) \tag{6}$$

It will be apparent that, as for the structure function (5), the terms with $j = k$ can be separated from the others, giving:

$$\begin{aligned} G(\mathbf{r}) &= \delta(\mathbf{r}) + \frac{1}{N}\sum_{i\neq j}\delta(\mathbf{r} + \mathbf{R}_j - \mathbf{R}_i) \\ &= \delta(\mathbf{r}) + \rho g_{pcf}(\mathbf{r}) \end{aligned} \tag{7}$$

which serves to define the pair correlation function (PCF), $g_{pcf}(\mathbf{r})$. Here ρ is the average atomic number density (typically expressed in units of atoms per Å^3). Formally there is a distinction between the pair distribution function (PDF), also sometimes called the radial distribution function (RDF), $g(r)$, and the PCF, $g_{pcf}(\mathbf{r})$, in that

$$g(r) = \langle g_{pcf}(\mathbf{r})\rangle_\Omega \tag{8}$$

where the average is over the directions of $\mathbf{r}$. In practice, for an isotropic material such as a powdered crystal, the two functions are identical unless there is some internal coordinate system, such as a molecule's coordinate axes or the coordinate axes associated with a surface, that can be defined.

If we now make the assumption (for the time being) that all the atoms in the material are the same type, and introducing (7) into (5), the sum over pairs of atoms in (5) is replaced by an integral over the pair correlation function:

$$\begin{aligned} F(\mathbf{Q}) &= f^{(\mathrm{IA})}(Q)^2 + \frac{1}{N}\sum_{j\neq k} f_j^{(\mathrm{IA})}(Q) f_k^{(\mathrm{IA})}(Q) \\ &\quad\times\quad \exp[i\mathbf{Q}\cdot(\mathbf{R}_j - \mathbf{R}_k)] \\ &= f^{(\mathrm{IA})}(Q)^2 + f^{(\mathrm{IA})}(Q)^2\rho\int g_{pcf}(\mathbf{r})\exp[i\mathbf{Q}\cdot\mathbf{r}]d\mathbf{r} \end{aligned} \tag{9}$$

For multicomponent materials, these expressions can be generalised to take account of the different atomic components present. This was first suggested by (Faber & Ziman, 1965) and the definitions used here are analogous to theirs throughout. Hence $g_{\alpha\beta}(\mathbf{r})$ would be the pair correlation function between atoms of type α and β. If there are J distinct atom types in the system, then the number of distinct pair correlation functions is $J(J+1)/2$.

IUCr macros version 2.1.4: 2010/12/07

The order in which α and β are specified is not important since by definition

$$g_{\alpha\beta}(\mathbf{r}) \equiv g_{\beta\alpha}(-\mathbf{r}) \tag{10}$$

from which it follows that

$$g_{\alpha\beta}(r) \equiv g_{\beta\alpha}(r) \tag{11}$$

In terms of these site-site correlation functions the autocorrelation function of the system would be defined as:

$$G(\mathbf{r}) = \sum_{\alpha} c_\alpha \delta(\mathbf{r}) + \rho \sum_{\alpha,\beta\geq\alpha} (2-\delta_{\alpha\beta}) c_\alpha c_\beta g_{\alpha\beta}(\mathbf{r}) \tag{12}$$

where $c_\alpha = \rho_\alpha/\rho$ and ρ_α is the number density of atoms of type α. The Kronecker $\delta_{\alpha\beta}$ is needed in (12) to avoid double counting pairs of atoms of the same type. The atomic fractions are needed to take account of the different percentages of the atom types present.

Using (12) the structure function is immediately generalised for multicomponent materials as in (9):

$$F(\mathbf{Q}) = \sum_{\alpha} c_\alpha f_\alpha^{(\mathrm{IA})}(Q)^2 + \sum_{\alpha\beta\geq\alpha} (2-\delta_{\alpha\beta}) \times c_\alpha c_\beta f_\alpha^{(\mathrm{IA})}(Q) f_\beta^{(\mathrm{IA})}(Q) S_{\alpha\beta}(\mathbf{Q}) \tag{13}$$

with the partial structure factors defined by

$$S_{\alpha\beta}(\mathbf{Q}) = \rho \int g_{\alpha\beta}(\mathbf{r}) \exp(i\mathbf{Q}\cdot\mathbf{r}) d\mathbf{r}, \tag{14}$$

which become

$$S_{\alpha\beta}(Q) = \langle S_{\alpha\beta}(\mathbf{Q}) \rangle_\Omega = 4\pi\rho \int r^2 g_{\alpha\beta}(r) \frac{\sin Qr}{Qr} dr \tag{15}$$

for an isotropic system.

Sometimes the site-site pair correlation function is written as a constant plus a fluctuation term:

$$g_{\alpha\beta}(\mathbf{r}) = 1 + h_{\alpha\beta}(\mathbf{r}) \tag{16}$$

with $h_{\alpha\beta}(\mathbf{r})$ the site-site *total* pair correlation function between atoms of type α and β.

The Fourier transform of a constant in r-space is a δ-function in Q. Hence, using (16), the partial structure factors become

$$S_{\alpha\beta}(\mathbf{Q}) = \rho\delta(\mathbf{Q}) + H_{\alpha\beta}(\mathbf{Q}) \tag{17}$$

where

$$H_{\alpha\beta}(\mathbf{Q}) = \rho \int h_{\alpha\beta}(\mathbf{r}) \exp(i\mathbf{Q}\cdot\mathbf{r}) d\mathbf{r} \tag{18}$$

or

$$H_{\alpha\beta}(Q) = 4\pi\rho \int_0^\infty r^2 h_{\alpha\beta}(r) \frac{\sin Qr}{Qr} dr \tag{19}$$

Note however that this $\delta(\mathbf{Q})$ function is rarely shown in the scattering equations since it is not observable in the experiment, so the terms $S_{\alpha\beta}(Q)$ and $H_{\alpha\beta}(Q)$ are used rather interchangably since they differ only at $Q = 0$.

Including these definitions in (15) leads to the final expression for the x-ray differential scattering cross section for an isotropic system:

$$F(Q) = \langle F(\mathbf{Q}) \rangle_\Omega = \sum_{\alpha} c_\alpha f_\alpha^{(\mathrm{IA})}(Q)^2 + \sum_{\alpha\beta\geq\alpha} (2-\delta_{\alpha\beta}) \times c_\alpha c_\beta f_\alpha^{(\mathrm{IA})}(Q) f_\beta^{(\mathrm{IA})}(Q) H_{\alpha\beta}(Q) \tag{20}$$

2.3. X-ray normalisation factor

As it stands, the x-ray differential scattering cross section, equation (20), represents, in real space, the convolution of the atomic centres radial distribution function with the broadening function caused by the electron distribution around each atom. As such it is not particularly helpful in helping to understand the arrangement of atom centres, since the electron distribution is quite broad. Hence it is traditional to divide this differential cross section by a "de-broadening" function, $B(Q)$, which represents the broadening due to the electron distribution, to produce an effective atomic x-ray structure factor (Warren, 1968):

$$S(Q) = F(Q)/B(Q), \tag{21}$$

This can only be done exactly within the independent atom approximation (i.e. assuming the x-ray form factor does not depend on the atomic arrangement) and for a single component material. If there are two or more atomic components, then their corresponding x-ray form factors have different Q dependencies in general, so that the correct form for this broadening function is unclear.

Frequently, the assumed broadening function is of the form

$$B(Q) = \left(\sum_{\alpha} c_\alpha f_\alpha(Q) \right)^2 \tag{22}$$

which represents the sum of the form factor terms outside the interference functions in (20). However in the event that all the structure factors go to zero ($H_{\alpha\beta}(Q) = 0$ for all Q), which would occur in a system with no correlations, then the residual term, $\sum_\alpha c_\alpha f_\alpha(Q)^2 / \left(\sum_\alpha c_\alpha f_\alpha(Q)\right)^2$ in (21) would still retain a variation with Q, except for the case of a single component system. This might not be a problem in general, but for structural modelling purposes this inherent Q variation for the uncorrelated system can drive the fit away from the best solution, (Soper, 2007).

This particular problem is alleviated if the the coherent self scattering is also used as the broadening fuction:

$$B(Q) = \left(\sum_{\alpha} c_\alpha f_\alpha(Q)^2 \right). \tag{23}$$

In the end the choice of which de-broadening function to use is up to the user.

3. Data corrections

The form (20) is of course never actually measured in real scattering experiments. The typical angle dispersive experiment

measures the number of x-rays scattered as a function of scattering angle into a detector of fixed solid angle for a specified wavelength. Energy dispersive measurements on the other hand fix the detector scattering angle and measure the scattering as a function of x-ray energy. In either case the x-rays will be subject to attenuation in the material from which they are scattering, and also there will be scattering and attenuation from any container of the material. They may be subject to multiple scattering in the material and its containment, and in addition there may be contributions (background) from any air and other items that may be in or near the x-ray beam.

The corrections for these effects have been known for a long time and will not be described in detail here. The methods used in GudrunX to perform the attenuation and multiple scattering corrections use a numerical solution of the required integrals and were developed from the following references: (Paalman & Pings, 1962; Kendig & Pings, 1965; Soper & Egelstaff, 1980; Vineyard, 1954; Blech & Averbach, 1965; Soper, 1983), and the x-ray scattering and capture cross sections are taken from the tabulations available at **http://ftp.esrf.eu/pub/scisoft/xop2.3/DabaxFiles/**. These in turn derive from tabulations of the x-ray form factor coefficients, (Waasmaier & Kirfel, 1995), Compton coefficients, (Balyuzi, 1975), and tables of the photon scattering, capture and photoelectron cross sections due to a variety or authors, (Pratt, 1960; Hubbell, 1969; Scofield, 1973; Hubbell, 1975; Hubbell, 1977*a*; Hubbell, 1977*b*; Hubbell & Overbo, 1979; Hubbell *et al.*, 1980; Saloman & Hubbell, 1986; Saloman & Hubbell, 1987). Note that although multiple scattering in x-ray experiments is often treated as negligible, this assumption is not always justified. If for example a particular sample scatters a fraction x of the beam which hits it, then it is reasonable to assume the multiple scattering will be a fraction $\bigcirc(x)$ of the single scattering. Even for the sub-millimetre sample sizes typical of x-ray scattering x can still be a significant fraction for materials containing heavier elements. Moreover since the same samples will have a pronounced angular dependence to the attenuation correction, the multiple scattering will also have a marked scattering angle dependence and so should not be ignored. In GudrunX the multiple scattering is calculated on the assumption that the single scattering is isotropic with scattering angle, but of course, for x-rays, this approximation is already questionable due to the marked angular dependence of the x-ray form factors, and a more rigorous procedure will eventually be implemented.

There are in addition a number of other corrections required which are specific to x-ray scattering. These include (in the present instance) Compton (inelastic) x-ray scattering, x-ray polarization, bremsstrahlung radiation and x-ray fluorescence, all of which can have a major impact on the measured data. Again these effects are understood and can be corrected for using simple procedures. The methods used to perform those corrections are less well-documented in general, and so the methods used in GudrunX are described here in some detail.

3.1. X-ray inelastic (Compton) scattering

For x-rays, inelastic scattering arises from individual electrons recoiling under the impact of the incident x-ray, giving rise to so-called "incoherent" scattering. This is a well understood problem, having been originally studied by (Compton, 1923), and then subsequently revisited (Breit, 1926; Dirac, 1926; Klein & Nishina, 1929). The Compton scattering can be calculated for each atom within the independent atom approximation (Hubbell *et al.*, 1975). The actual impact on the diffraction data is not quite so clear cut, since both the Compton scattering level and accompanying Breit-Dirac correction factor are affected by the energy response of the detector, and this is not always known precisely. It is generally accepted that the Klein-Nishina formulation for the incoherent differential cross section of a stationary free electron for an unpolarised incident x-ray beam is the correct one, (Read & Lauritsen, 1934):

$$\left(\frac{d\sigma}{d\Omega}\right)_{\rm KN} = \frac{1}{2}P(\gamma,\theta)^2\left[P(\gamma,\theta)+P(\gamma,\theta)^{-1}-1+\cos^2 2\theta\right] \tag{24}$$

where

$$P(\gamma,\theta) = \frac{1}{\left(1+2\gamma\sin^2\theta\right)}. \tag{25}$$

Note that the scattering angle in these equations is 2θ as before, while γ is the ratio of incident photon energy to rest mass energy of the electron.

At the relatively low ($\lesssim$ 100keV) incident x-ray energies that are used in x-ray diffraction the electrons are of course bound to the atoms, so cannot be regarded as free, particularly at small Q. As a result the inelastic scattering is actually zero at $Q = 0$ and grows with increasing Q eventually reaching a plateau where all Z electrons on the atom are scattering incoherently. As a result the Klein-Nishina formula needs to be corrected for the initial states of the electrons:

$$\left(\frac{d\sigma}{d\Omega}\right)_{incoh} = \left(\frac{d\sigma}{d\Omega}\right)_{\rm KN} S(x,Z) \tag{26}$$

where $x = Q/4\pi$ and $S(x,Z)$ is an incoherent form factor which needs to be estimated.

The calculation of this form factor, of which there is one for each element, can be achieved in at least two ways. The standard method, (Hubbell *et al.*, 1975), involves a summation over the ground state electron wave functions, typically using the self-consistent Hartree-Fock method. Alternatively it is possible to use the impulse approximation and use the Compton profile (electron momentum distribution), (Ribberfors, 1983) to achieve the same result to good accuracy. We simply note here that $S(x,Z)$ can be expressed as a series, (Balyuzi, 1975):

$$S(x,Z) = Z - \sum_{i=1}^{5} a_i \exp\left(-b_i x^2\right), \tag{27}$$

which is useful when it is needed to calculate the Compton scattering at arbitrary values of Q. Note that at large Q (=large x) $S(x,Z) \longrightarrow Z$, but the actual scattering will fall below this limit due to the electron recoil term in the Klein-Nishina formula. It should also be borne in mind, that these expressions

IUCr macros version 2.1.4: 2010/12/07

do not include the effect of variable detector efficiency with x-ray energy in the calculation. Hence for anything other than a "black" x-ray detector (meaning that it counts all photons with equal efficiency irrespective of their energy) the results will not be accurate. In practice it is quite hard to build such a detector.

Compton scattering is zero at $Q = 0$, and grows with increasing Q. Meanwhile the x-ray form factors which control the amplitude of the distinct scattering rapidly diminish with increasing Q. This means at high Q the x-ray diffraction data are dominated by the Compton scattering which forms a background that has to be subtracted in order to get to the structurally important distinct scattering. This introduces a systematic uncertainty to extracted coherent x-ray data that gets progressively worse the higher the value of Q. As will be seen in the next section, the normalisation of x-ray data onto an absolute cross section scale relies on knowing the high Q data to good accuracy.

3.2. Data calibration for x-rays

The method adopted in GudrunX for putting the raw x-ray counts onto an absolute scale of scattering cross section is that developed by (Krogh-Moe, 1956) and (Norman, 1957).

Putting together the results from equation (20) and section 3.1, the total differential scattering cross section for x-rays is:

$$\begin{aligned}\left(\frac{d\sigma}{d\Omega}\right)_x &= \left(\frac{d\sigma}{d\Omega}\right)_{Th}(\lambda,2\theta)F_x(Q) + \left(\frac{d\sigma}{d\Omega}\right)_{KN}\sum_\alpha c_\alpha S(x,Z_\alpha)\\ &= \sum_\alpha c_\alpha\left[\left(\frac{d\sigma}{d\Omega}\right)_{Th} f_\alpha^2(Q) + \left(\frac{d\sigma}{d\Omega}\right)_{KN} S(x,Z_\alpha)\right]\\ &+ \left(\frac{d\sigma}{d\Omega}\right)_{Th}\sum_{\alpha\beta\geq\alpha}(2-\delta_{\alpha\beta})\,c_\alpha c_\beta f_\alpha(Q) f_\beta(Q) H_{\alpha\beta}(Q)\\ &= \left(\frac{d\sigma}{d\Omega}\right)_{self}\\ &+ \left(\frac{d\sigma}{d\Omega}\right)_{Th}\sum_{\alpha\beta\geq\alpha}(2-\delta_{\alpha\beta})\,c_\alpha c_\beta f_\alpha(Q) f_\beta(Q) H_{\alpha\beta}(Q)\end{aligned} \tag{28}$$

where the Thomson differential scattering cross section for an unpolarized incident x-ray is

$$\left(\frac{d\sigma}{d\Omega}\right)_{\rm Th} = \frac{1}{2}\left[1+\cos^2 2\theta\right]. \tag{29}$$

Equation (28) serves to define the self differential scattering cross section for x-rays,

$$\left(\frac{d\sigma}{d\Omega}\right)_{self} = \sum_\alpha c_\alpha\left[\left(\frac{d\sigma}{d\Omega}\right)_{Th} f_\alpha^2(Q) + \left(\frac{d\sigma}{d\Omega}\right)_{KN} S(x,Z_\alpha)\right] \tag{30}$$

while the distinct scattering is given by

$$\begin{aligned}\left(\frac{d\sigma}{d\Omega}\right)_{distinct} &= \left(\frac{d\sigma}{d\Omega}\right)_{Th}\sum_{\alpha\beta\geq\alpha}(2-\delta_{\alpha\beta})\,c_\alpha c_\beta f_\alpha(Q) f_\beta(Q)\\ &\times H_{\alpha\beta}(Q)\end{aligned} \tag{31}$$

The underlying idea is that the Fourier inverse of equation (18) is given by

$$h_{\alpha\beta}(\mathbf{r}) = \frac{1}{2\pi^2\rho}\int H_{\alpha\beta}(\mathbf{Q})\exp(i\mathbf{Q}\cdot\mathbf{r})d\mathbf{Q} \tag{32}$$

so that for $\mathbf{r} = 0$

$$\begin{aligned}h_{\alpha\beta}(0) &= \frac{1}{2\pi^2\rho}\int H_{\alpha\beta}(\mathbf{Q})d\mathbf{Q}\\ &= \frac{1}{2\pi^2\rho}\int_0^\infty Q^2 H_{\alpha\beta}(Q)dQ\end{aligned} \tag{33}$$

Assuming $g_{\alpha\beta}(0) = 0$ (no atomic overlap) then $h_{\alpha\beta}(0) = -1$, i.e. equation (33) has a known value.

Suppose, using the procedures described in this chapter, we obtain $\left(\frac{d\sigma}{d\Omega}\right)_x(\lambda,2\theta)$ within our calibration factor, C, namely the number of x-ray counts per measuring channel after background subtraction is $I_x(\lambda,2\theta) = C\left(\frac{d\sigma}{d\Omega}\right)_x(\lambda,2\theta)$. Performing the integrals (33) on these data (bearing in mind of course that Q is a function of θ) we obtain

$$\begin{aligned}\int_{Q_{min}}^{Q_{max}} Q^2\left[\frac{I_x(\lambda,2\theta)}{\left(\frac{d\sigma}{d\Omega}\right)_{Th}(\lambda,2\theta)}\right]dQ =\\ C\int_{Q_{min}}^{Q_{max}} Q^2\left[\frac{\left(\frac{d\sigma}{d\Omega}\right)_{self}(\lambda,2\theta)}{\left(\frac{d\sigma}{d\Omega}\right)_{Th}(\lambda,2\theta)}\right]dQ\\ +C\sum_{\alpha\beta\geq\alpha}(2-\delta_{\alpha\beta})\,c_\alpha c_\beta\\ \times\int_{Q_{min}}^{Q_{max}} Q^2 f_\alpha(Q) f_\beta(Q) H_{\alpha\beta}(Q)dQ\end{aligned} \tag{34}$$

The approximation that Krogh-Moe and Norman make is that

$$\frac{1}{2\pi^2\rho}\int_{Q_{min}}^{Q_{max}} Q^2 f_\alpha(Q) f_\beta(Q) H_{\alpha\beta}(Q)dQ = -Z_\alpha Z_\beta \tag{35}$$

as per (33). Given that the electron cloud around each atom is diffuse, and especially within the independent atom approximation, which states that the electron cloud is independent of the surrounding atoms, there is no guarantee this condition is exact, particularly since the integral can only be performed over a finite Q range. Hence within GudrunX there is the opportunity to add an arbitrary constant to this value, so allowing for possible electron overlap between neighbouring atoms. The revised version of the Krogh-Moe and Norman condition is

$$\frac{1}{2\pi^2\rho}\int_{Q_{min}}^{Q_{max}} Q^2 f_\alpha(Q) f_\beta(Q) H_{\alpha\beta}(Q)dQ = -Z_\alpha Z_\beta + \delta \tag{36}$$

where δ is set by the experimenter. Clearly it would make sense that $\delta \geq 0$ (electron densities cannot be negative). Inserting (36) into (34) and since all the terms on the right-hand side of (34) are calculable (apart from C), then in principle C can

be determined by straightforward inversion of (34). In practice, since corrections for attenuation, multiple scattering, polarisation, bremsstrahlung scattering, and fluorescence (see later sections) have to be performed on the data, the calibration constant has to be determined iteratively at the end of each pass through the data. Five such iterations is generally found to be enough to give a stable value of the calibration constant.

3.3. X-ray polarisation corrections

This has already been alluded to in the discussion of x-ray inelastic scattering, Section 3.1. There, mention was made of the fact that both the Thomson, (29), and Klein-Nishina, (24), scattering formulae apply to an unpolarised incident x-ray beam. The polarisation correction arises because an x-ray, being a transverse wave, is scattered by that component of its electric wave vector which is at right angles to its direction of travel. Hence an x-ray scattered at 0° or 180° can be scattered whatever its polarisation because the right angle condition is always satisfied, but for an x-ray scattered at 90° in the horizontal plane, only the vertical component of its electric field vector can scatter, so the intensity drops to 1/2 of its zero angle value. This is what leads to the Thomson formula, (29).

As far as we know a laboratory x-ray source is unpolarised, so the Thomson formula should work fine in that case, but with synchrotron x-ray sources, the radiation in the plane of the orbit is horizontally polarised, so that if the detectors move in the vertical plane, as is normally the case, there will be no discernible polarisation effect. At synchrotron instruments the polarization of the beam (after mirrors and monochromators) is often measured directly by looking at the scattering from a piece of Kapton, which would normally be expected to be isotropic in an unpolarized beam.

GudrunX allows for the possibility that the incident beam may be polarised. This case was dealt with in detail by (Kahn *et al.*, 1982) for the case of single crystal reflections by a polarised incident beam. Specifically they showed that the polarisation correction for a particular reflection is given by:

$$P(2\theta) = \frac{1}{2}\left[1 + \cos^2(2\theta) - \phi\cos(2\chi)\sin^2(2\theta)\right] \qquad (37)$$

where ϕ is a measure of the degree of polarisation of the incident beam:

$$\phi = \frac{E_H^2 - E_V^2}{E_H^2 + E_V^2}, \qquad (38)$$

E_H, E_V are the horizontal and vertical components of the electric field vector, with horizontal defined as the scattering plane at right angles to the axis about which the detector rotates, vertical is perpendicular to this plane, and χ is the azimuthal angle of the detecting element out of the horizontal plane. $\phi = 0$ means the horizontal and vertical components of the incident polarisation are equal, corresponding to an unpolarised beam, while $\phi = -1$ corresponds to incident polarisation at right angles to the scattering plane. If $\chi = 0$ and $\phi = -1$ then there will be no polarisation correction. If $\phi = +1$ this corresponds to incident polarisation in the horizontal plane, which means that for $2\theta = 90°$ there will no scattering. Clearly ϕ and χ play equivalent roles in this formula, and in practice, for unpolarised x-rays we should set both values to zero.

In GudrunX the polarisation correction is applied after subtracting any fluorescent scattering, and after correcting the scattering data for backgtound, multiple scattering, container scattering and attenuation. The bremsstrahlung correction (see next section) is performed after the polarisation correction since no calculation of polarisation is included in the estimate of the bremsstrahlung scattering. The iterative estimate of the overall calibration factor is also made after the polarisation correction since the calculation described in section 3.2 makes no allowance for x-ray polarisation.

3.4. Bremsstrahlung scattering

In addition to the usual electron transition lines, K_α, K_β, and so on, laboratory x-ray tubes produce a general background bremsstrahlung radiation caused by the incident electrons being slowed down in the anode material. This has a characteristic spectrum whose maximum energy corresponds to the electron bombardment energy, E_e, (McCall, 1982):

$$C\left(\frac{E_e}{E_x} - 1\right)^{\alpha} \quad E_x \leqslant E_e \qquad (39)$$

where C is a constant that depends on the atomic number of the target nucleus and $\alpha \approx 1$. In practice this spectrum will be self attenuated by the target material, so assuming the x-rays have to travel on average a distance, L_T through the anode material before being emmitted, the spectrum will be modified by a factor $\exp\left(-\mu_T\left(E_x\right)L_T\right)$, where $\mu_T\left(E_x\right)$ is the attenuation coefficient of the target material. Futhermore it is normal, in an attempt to reduce unwanted counts reaching the detector, to place a suitable absorbing foil that will stop the K_β radiation. This will introduce its own transmittance factor on the incident beam, $\exp\left(-\mu_F\left(E_x\right)L_F\right)$, where $\mu_F\left(E_x\right)$ and L_F are the attenuation coefficient and thickness of the absorbing foil respectively. Finally it is expected that the detecting system will impose its own cut-off in energy, determined by the discriminating system on the detector. To represent this we use the function $1\Big/\left(1+\exp\left(\frac{E_0-E_x}{w}\right)\right)$, where E_0 is the cut-off energy and w is the width of the cut-off. Hence the overall assumed expression for the bremsstrahlung radiation is given by

$$I_{Br}\left(E_x\right) = C_{Br}\exp\left[-\mu_T\left(E_x\right)L_T\right]\left(\frac{E_e}{E_x} - 1\right)^{\alpha} \times \exp\left[-\mu_F\left(E_x\right)L_F\right]\frac{1}{\left(1+\exp\left(\frac{E_0-E_x}{w}\right)\right)} \qquad (40)$$

For the purposes of data analysis the (arbitrary) constant of proportionality C_{Br} is chosen so that $\int_0^{E_e} I_{Br}\left(E_x\right)dE_x = 1$.

Obviously if the diffractometer has a monchromator, the bremsstrahlung correction is not necessary, but otherwise, because bremsstrahlung radiation produces a spread of x-ray wavelengths it has the effect of producing a smeared out version of the structure factor being sought. This smeared out version must be subtracted from the total differential scattering cross section in order to get to the true differential cross section for

IUCr macros version 2.1.4: 2010/12/07

the specified x-ray wavelength. Fig. 1 shows an example of what the resulting incident bremsstrahlung spectrum might look like using this formula.

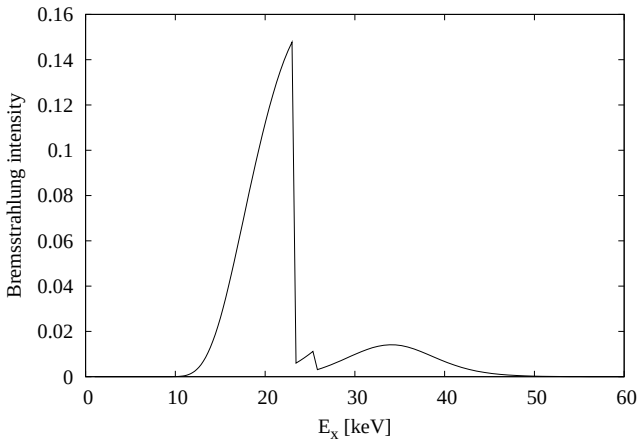

Figure 1
Example of the estimated bremsstrahlung spectrum for a silver (Ag) source running at $E_e = 60$keV and assuming a Rh filter of thickness 0.05mm is used. The penetration depth in the Ag anode is assumed to be 0.03mm, and the high energy detector cut-off, E_0, was set at 36keV with a spread (w) of 3keV. The sharp edge near $E_x = 23$keV is caused by the Rh K_α edge, while the smaller edge near $E_x = 25$keV comes from the Ag anode material. Use of the Rh filter prevents most silver K_β x-rays reaching the sample.

To use this spectrum in the data analysis, it is necessary to convolute the bremsstrahlung spectrum with the differential scattering cross section. After all the corrections and in the presence of bremsstrahlung radiation, the observed total differential cross section, $\left(\frac{d\sigma}{d\Omega}\right)_t(\lambda, 2\theta)$ is given by

$$\left(\frac{d\sigma}{d\Omega}\right)_t(\lambda, 2\theta) = \left(\frac{d\sigma}{d\Omega}\right)_x(\lambda, 2\theta) + f_{br}\left[\left(\frac{d\sigma}{d\Omega}\right)_x(\lambda, 2\theta) \bigotimes I_{br}(E_x)\right] \quad (41)$$

where f_{br} is the fraction of the total scattering that comes from bremsstrahlung radiation. It has to be determined by the user: if too much bremsstrahlung scattering is subtracted, then the $\left(\frac{d\sigma}{d\Omega}\right)_x(\lambda, 2\theta)$ that is extracted will go negative in some regions, which is unphysical. Therefore f_{br} can be regarded as a fitting factor, but it should be the same for all samples, and is determined once for a particular instrument configuration using a standard sample such as powdered silica.

Since $\left(\frac{d\sigma}{d\Omega}\right)_x(\lambda, 2\theta)$ is not known at the outset it has to be found iteratively. Suppose at the beginning of the n^{th} iteration our current estimate for $\left(\frac{d\sigma}{d\Omega}\right)_x(\lambda, 2\theta)$ is $\left(\frac{d\sigma}{d\Omega}\right)_x^{(n-1)}(\lambda, 2\theta)$. Using (41) the next estimate will be:

$$\left(\frac{d\sigma}{d\Omega}\right)_x^{(n)}(\lambda, 2\theta) = \frac{\left(\frac{d\sigma}{d\Omega}\right)_t(\lambda, 2\theta) - f_{br}\left[\left(\frac{d\sigma}{d\Omega}\right)_x^{(n-1)}(\lambda, 2\theta) \bigotimes I_{br}(E_x)\right]}{(1 - f_{br})}. \quad (42)$$

For the first iteration, $n = 1$, it is natural to set $\left(\frac{d\sigma}{d\Omega}\right)_x^{(0)}(\lambda, 2\theta) = \left(\frac{d\sigma}{d\Omega}\right)_t(\lambda, 2\theta)$ to start the sequence off. Note that when performing the convolution in (41) and (42) it is necessary to include the sample attenuation factor at each energy in the bremsstrahlung spectrum, since these attenuation factors vary markedly with energy.

Using the bremstrahlung spectrum shown in Fig. 1, Fig. 2 shows the extracted $\left(\frac{d\sigma}{d\Omega}\right)_x(\lambda, 2\theta)$, the single atom scattering, and the convoluted bremstrahlung spectrum for Si powder measured on a Ag tube x-ray source. Fig. 3 shows the structure factors, after dividing by the single atom scattering ($\sum_\alpha c_\alpha f_\alpha^{(\mathrm{IA})}(Q)^2$), obtained with and without the bremsstrahlung correction. It is seen that including the bremsstrahlung contribution makes a big difference to the peak heights, and makes the peak profile cleaner and more symmetric. In addition the background on the data is much flatter when the bremsstrahlung is subtracted. Obviously by measuring or otherwise improving the bremsstrahlung spectrum used in these calculations, these results might be improved still further.

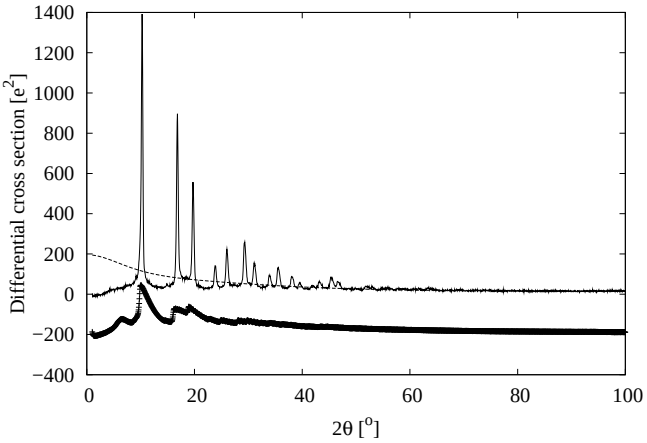

Figure 2
Extracted x-ray differential scattering cross section (solid line) for Si powder using Ag K_α radiation with a Rh filter. The dashed line shows the estimated single atom scattering plus Compton scattering and the crosses show the convolution of the differential cross section with the bremsstrahlung spectrum from Fig. 1. The bremsstrahlung factor, f_{br}, was set to 0.5 for this calculation.

IUCr macros version 2.1.4: 2010/12/07

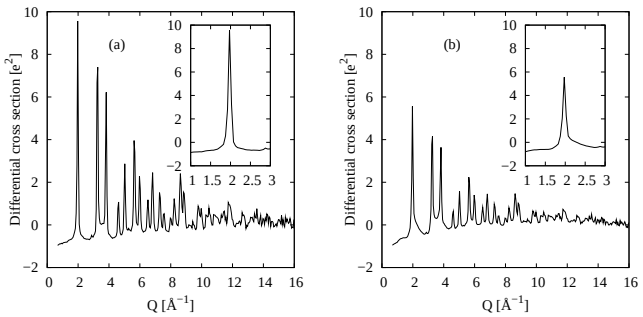

Figure 3
Comparison of extracted x-ray structure factors (differential cross section divided by single atom scattering) for Si powder, assuming the bremsstrahlung factor is 0.5 (a), or 0.0 (b). The insets show the first peak under the same conditions. Notice how the peak in (a) becomes sharper as a result of the bremsstrahlung deconvolution and loses the long tail to higher Q which was present in the original version (b).

3.5. X-ray fluorescence corrections

X-ray fluorescence occurs when an x-ray is absorbed, exciting an electron, but the electron subsequently then decays into a different orbital, emitting a different radiation wavelength than that which caused the excitation. There is a (small) time delay in this process. Fluorescence will be a problem whenever there is a fluorescing electron transition near the energy of the incident x-ray. Fluorescence becomes obvious in the data analysis by making it impossible to normalise to the single atom scattering plus Compton scattering in a satisfactory manner.

Traditionally it is assumed fluorescence is a background constant with scattering angle (Klug & Alexander, 1954) because the fluorescent x-ray can be emitted in any direction. This would be true if the sample did not attenuate the beam at all, but in practice, particularly with the heavily absorbing samples that are likely to fluoresce, the attenuation effect is not uniform with scattering angle, and since the fluorescent x-ray will be of a lower energy than the exciting x-ray, the effect of attenuation in the incident and scattered path needs to be included in the calculation. In GudrunX it is assumed that an element, e, will fluoresce above a characteristic x-ray energy or wavelength, called its fluorescence energy, $E_f^{(e)}$. There are probably few if any cases of a single element fluorescing at more than one energy for a given incident spectrum so only one fluorescence energy is allowed per element. This is because typically it is the K edge in the absorption spectrum that fluoresces, while the L edge is at too low an energy to cause observable fluorescence. However, for the heavier elements it may be the L edge that fluoresces, in which case the corresponding K edge is probably at too high an energy to be excited by the incident x-ray spectrum.

It is expected that the fluorescing x-ray will be emitted isotropically in all directions with an intensity proportional to the known photoelectron cross-section for a given incident wavelength. However, the observed fluorescence intensity will also be affected by the incident x-ray spectrum - this is assumed to be the same as that used to calculate the bremsstrahlung correction, namely $(1 - f_{br})\delta(E_x - E_{K_\alpha}) + f_{br}I_{br}(E_x)$, and attenuation in the sample, which in turn depends on the incident x-ray energy, E_x, and the fluorescence energy. Hence it is necessary to calculate the attenuation factor in the sample (plus any containers) for an incident x-ray photon at a series of energies above the fluorescence energy with the emerging photon at the fluorescence energy. These "inelastic" attenuation factors, $A(E_x, E_f^{(e)}, 2\theta)$, are therefore distinct from the elastic attenuation factors that have been discussed hitherto, and have to be calculated separately. The sample fluorescence will also depend on the incident intensity at any given energy. If more than one element in the sample fluoresces, it is possible to assign relative weights, w_e, to those elements when calculating the fluorescence scattering. Finally, since it is impossible to assign an absolute scale to this fluorescence scattering, the contribution of fluorescence is represented as a user-specified fraction, f_f, of the sample (elastic) scattering integrated over all scattering angles.

To summarise, the fluorescence is calculated in GudrunX according to the formula:

$$\begin{aligned} I_f(2\theta) = f_f \sum_e w_e \\ \times \int_{E_f^{(e)}} [(1 - f_{br})\delta(E_x - E_{K_\alpha}) + f_{br}I_{br}(E_x)] \\ \times \sigma_{PE}^{(e)}(E_x) A(E_x, E_f^{(e)}, 2\theta) dE_x \end{aligned} \quad (43)$$

where the sum is over the elements in the sample, and $\sigma_{PE}^{(e)}(E_x)$ is the photoelectron cross section at energy E_x for element e. The normalising constant f_f is chosen so that the $\int I_f(2\theta)d2\theta$ is a user-defined fraction of $\int \left(\frac{d\sigma}{d\Omega}\right)_t (\lambda, 2\theta)d2\theta$, and the user has to choose the appropriate fluorescence energy and weight for each element as needed.

This fluorescence scattering is subtracted from the observed x-ray scattering data as a function of scattering angle prior to any processing in terms of normalisation, correction for attenuation and multiple scattering, and background or container subtractions. Fig. 4 gives examples of what happens when the fluorescence correction is applied, (a), and when it is not applied, (b).

IUCr macros version 2.1.4: 2010/12/07

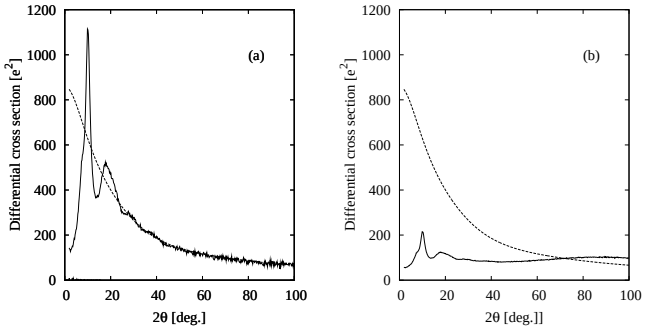

Figure 4
Comparison of extracted x-ray differential cross section for a sodium tellurite glass powder, assuming the fluorescence fraction is 0.75 (a), or 0.0 (b). The assumed fluorescence energy of Te was 31.2keV.

4. Program details

Figure 5 gives an overview of the sequence of operations that is performed by Gudrun X. The GudrunX program is written as a JAVA™Graphical User Interface (GUI), which means that the software can be run on a wide variety of platforms, including Windows, Linux, Unix, Mac, etc. The GUI has a simple "tabbed pane" structure for the different elements of the analysis. The titles of these tabs are INSTRUMENT, BEAM, NORMALISATION, SAMPLE BACKGROUND, SAMPLE and CONTAINER. The SAMPLE and CONTAINER tabs can be given individual names to help identify them, and it is possible to include an indefinite number of SAMPLEs or SAMPLE and CONTAINER combinations. Each SAMPLE is allowed up to three CONTAINERs to allow for the possibility of multiple containements, such as heating elements, radiation shields and vacuum windows, etc. Each is used to define parameters for the corresponding parts of the experiment. A detailed user manual is available to describe both GudrunX and her sister program, GudrunN, which performs a similar function for neutron total scattering data. Figure 6 shows the appearance of this GUI on start up, while Figure 7 shows the SAMPLE tab after loading some data. The NORMALISATION tab allows the user to define whether they want the final output differential cross section to be remain un-normalised, or whether it should be normalised according to (22) or (23).

Currently two types of x-ray data file are supported, namely the XRDML format, based on the XML language, generated by PANalytical software, and the standard (x, y, e) format typically obtained at synchrotron sources. Other formats can be incorporated if there is a demand for them. Of course it is straightforward to switch off the Compton, polarisation, bremsstrahlung and fluorescence corrections if these are not needed for particular experimental arrangements.

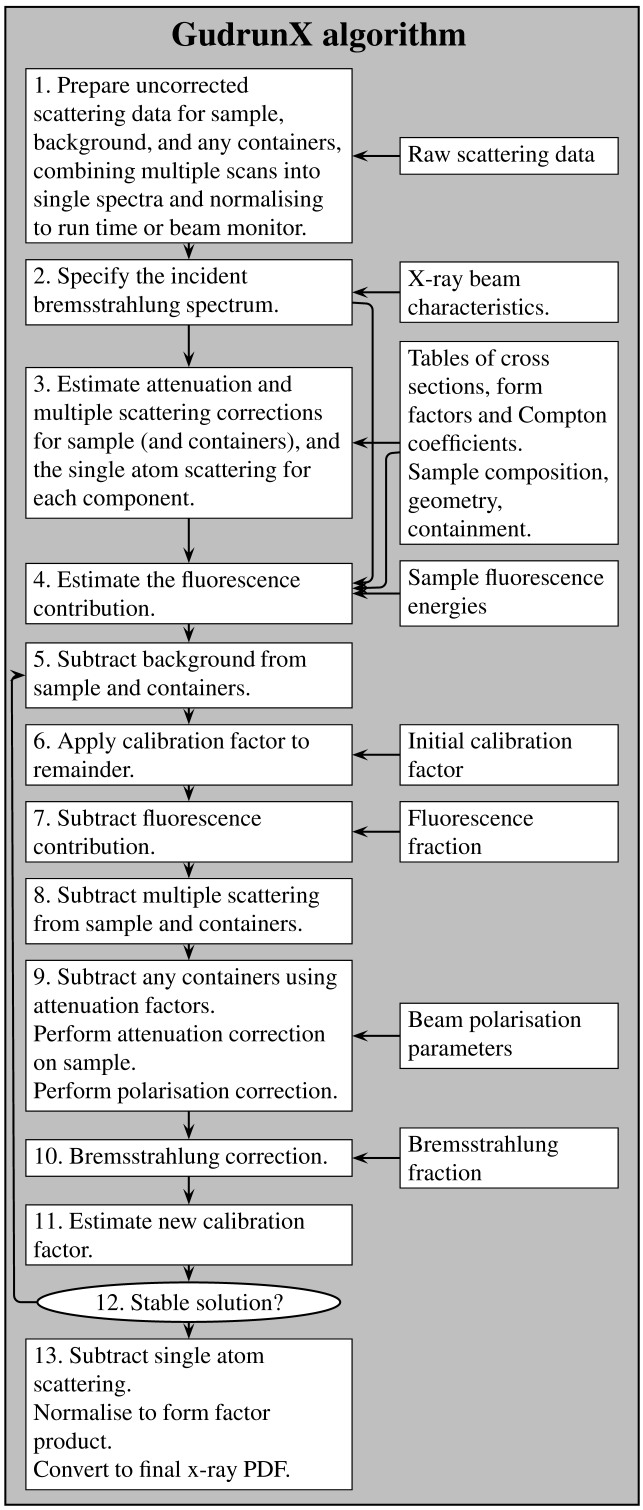

Figure 5
List of the primary steps in data analysis performed by GudrunX. Items on the right are the main inputs supplied by the user.

IUCr macros version 2.1.4: 2010/12/07

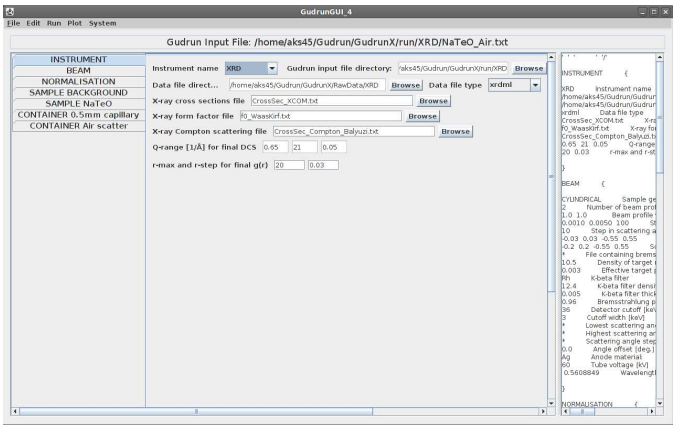

Figure 6
View of the GudrunX graphical user interface showing the INSTRUMENT tab on start up. SAMPLE BACKGROUND, SAMPLE and CONTAINER tabs can be added indefinitely as needed. A box on the right hand side lists all the parameters of the current input file. This input file is used to store and view these parameters but is not involved in the data analysis itself.

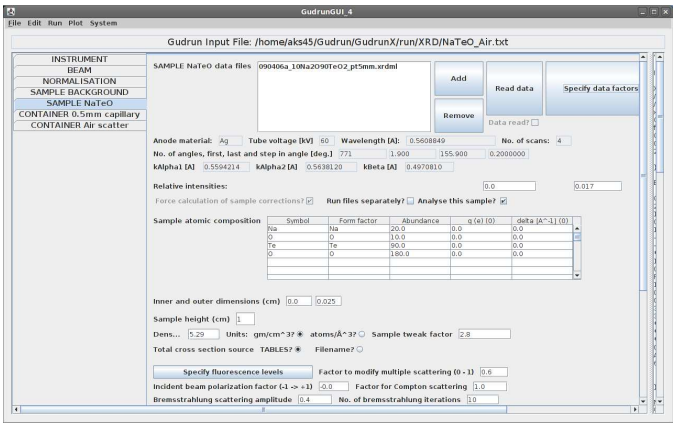

Figure 7
View of the GudrunX graphical user interface showing the SAMPLE tab after loading the data file for a particular sample.

The bulk of the processing is done via JAVA™methods which sit behind the GUI: for the typical datasets that are processed by the program these methods are mostly fast, even when several iterations of the bremsstrahlung convolution or the fluorescence calculation are required. The only non-JAVA™routines are the programs used to calculate the attenuation and multiple scattering corrections, which derive from much earlier Fortran codes written for neutron data analysis, as described in Section 3 above, and the Fourier transform code, described in Section 5, which is a standalone routine that can be applied to any dataset.

A simple graphics capability is provided by the GUI writing Gnuplot script files which can be subsequently plotted from the GUI. This allows the user to inspect the output at various stages of the data analysis. Because the primary graphical output is via Gnuplot this package is extremely versatile in plotting in a variety of graphical formats. However, the output data also appear in a simple multicolumn ASCII format so can be read directly into many other graphical packages.

5. Converting structure factor to pair distribution function (PDF)

GudrunX provides a facility to perform a Fourier transform on the extracted structure factors. The method adopted follows closely that of the top hat convolution method described in (Soper, 2009), but for completeness will be described here in detail. The basic assumption is that due to the fact that the data analysis may not have proceeded perfectly, the structure factor is on some kind of slowly varying Q-dependent background. This needs to be removed prior to Fourier transform if significant truncation oscillations are not to be generated. The background is generated by convolution of the data with the top hat function:

$$I'(Q) = \int_{Q_T} I(|\mathbf{Q} - \mathbf{Q}'|)\, T(\mathbf{Q}')\, d\mathbf{Q}' \qquad (44)$$

where the integral proceeds over all of reciprocal space for which the data exist, and the top hat function $T(\mathbf{Q})$ is given by:

$$\begin{aligned} T(\mathbf{Q}) &= \frac{3}{4\pi Q_T^3}, \quad |\mathbf{Q}| \le Q_T \\ &= 0, \qquad |\mathbf{Q}| > Q_T \end{aligned} \qquad (45)$$

The effect of the convolution therefore is to smear $I(Q)$ only in the region near $Q \pm Q_T$.

The next step is to take the Fourier transformation of the difference

$$D'(Q) = I(Q) - I'(Q) \qquad (46)$$

instead of Fourier transforming the intensity function itself, $I(Q)$, namely:

$$d(r) = \frac{1}{(2\pi)^3 \rho} \int_{Q_{min}}^{Q_{max}} D'(Q)) \exp[i\mathbf{Q}\cdot\mathbf{r}]\, d\mathbf{Q} \qquad (47)$$

where Q_{min}, Q_{max} is the range of Q values for which data are available. Making the use of the fact that the Fourier transform of a convolution is the product of the respective Fourier transforms, and noting that, following (30) and (31), the total intensity can be divided into *self* and *distinct* terms, $I(Q) = I_{self}(Q) + I_{distinct}(Q)$ it is straightforward to show that

$$d(r) = [G_{self}(r) + h_{distinct}(r)]\,(1 - f(Q_T r)) \qquad (48)$$

where

$$G_{self}(r) = \frac{1}{2\pi^2 \rho r} \int_{Q_{min}}^{Q_{max}} Q I_{self}(Q) \sin(Qr)\, dQ \qquad (49)$$

$$h_{distinct}(r) = \frac{1}{2\pi^2 \rho r} \int_{Q_{min}}^{Q_{max}} Q I_{distinct}(Q) \sin(Qr)\, dQ \qquad (50)$$

and

$$f(x) = \frac{3}{x^3}[\sin x - x\cos x] \qquad (51)$$

IUCr macros version 2.1.4: 2010/12/07

The function $1-f(x)$ is shown in Fig. 8. It is close to zero at low x, then rises close to unity for $x >\sim 4$. In other words it will heavily suppress low frequency structure in Q-space, but leave the higher frequency structure relatively intact. Precisely which frequency is cut off depends on the value of Q_T. For $x << 1$ $f(x) \approx x^2/10$ so that for small enough r and Q_T the structure in $d(r)$ at a distance of say $r = r_0$ will be 4 times more suppressed than structure at $r = 2r_0$ and so on.

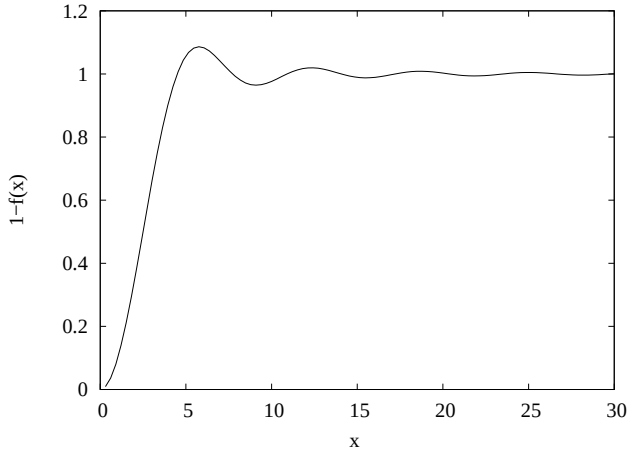

Figure 8
The convolution function $1-f(x)$ which is defined in equation (51).

Written in the form (48), it will be apparent that the convolution can easily be reversed in r space because the result (47) simply needs to be divided by $(1-f(Q_T r))$. By itself, however, this would achieve little since it would lead to the same function as would be derived by direct Fourier transform of the data. Instead the technique is to introduce a second constraint at this point and assume that for some $r < r_{min}$ we know $g(r)$ precisely, i.e. $g(r) = g_0(r)$ while for larger r, $g(r)$ is derived by inverting the convolution in (48):

$$\begin{aligned} d_{distinct}(r) &= g_0(r) - 1\,, \quad r < r_{min} \\ &= d(r)/(1-f(Q_T r))\,, \quad r \geq r_{min} \end{aligned} \tag{52}$$

The assumption here is that $G_{self}(r)$ makes an insignificant contribution for $r \geq r_{min}$. If it does make a contribution in this region then the present method will not remove it, but it will remove it for $r < r_{min}$.

The object is to obtain an interference function in Q space which has minimal contributions from the self scattering background and which satisfies our specified constraints at r_{min}. In principle one could simply Fourier transform (52) back to Q space to achieve this, but if $g(r)$ is structured to high r doing so might introduce further truncation effects. In addition unless the reverse transform is done carefully, this procedure will lose the statistical quality of the original data. A better plan is to generate an additional background function, $b(r)$, such that the function

$$d_{distinct}(r) = d(r) - b(r) \tag{53}$$

This leads to

$$\begin{aligned} b(r) &= d(r) - g_0(r) + 1, \quad r < r_{min} && (54) \\ &= -d(r)\, f(Q_T r)/(1-f(Q_T r))\,, \quad r \geq r_{min} && (55) \end{aligned}$$

Fourier transforming this to Q leads to:

$$B(Q) = 4\pi\rho \int r^2 b(r) \frac{\sin Qr}{Qr} dr \tag{56}$$

This extra background in Q space is then subtracted from $D'(Q)$ to yield an estimate of the interference differential cross section:

$$I_{int}^{(distinct)}(Q) = I(Q) - I'(Q) - B(Q) \tag{57}$$

Because the function $f(Q_T r)$ is short ranged in r the likelihood of truncation oscillations being transferred to $B(Q)$ is small. By this method the statistical quality of the original data is left intact, the specified constraint that $g(r)$ must adopt some known form $g_0(r)$ for $r < r_{min}$, and the effects of truncation in both Q and r-spaces are held to a minimum, even when the data have a large self scattering component.

Setting the width of the top hat function, Q_T, can be tricky since if the data have a rapidly varying background component then it would be desirable to make Q_T small to follow the shape of the background accurately. However when applied to (55) if the product $Q_T r_{min} \lesssim 3$ then the denominator is likely introduce a large spike at the cut-off, r_{min}. To avoid this, a useful rule of thumb is to set $Q_T > \dfrac{3}{r_{min}}$, but in the end if the data have a background which varies rapidly with Q there will always be a limit to how much useful information can be extracted from them.

In those cases where the background variation with Q is very slow, an alternative to the initial top hat convolution, (44), is to simply define a scattering level based on the large Q data and subtract this level from the data prior to the Fourier transform, (47). Subsequently the analysis proceeds as above, except that the convolution function, (51), is zero over all x. Any slow variation in the background is then removed by the requirement that the value of $g(r)$ for $r < r_{min}$ is assumed to be known. Either option is available in the current version of GudrunX.

Figure 9 shows the structure factor and radial distribution function extracted using GudrunX for a 3mm diameter solid rod of amorphous silica and gives a sense of the quality of the data analysis that can be obtained with the above procedures. The small peak in $g(r)$ below the main peak at ~ 1.6Å is almost certainly a consequence of a mismatch between the independent atom form factors assumed for these data and the true (unknown) form factors for this material.

IUCr macros version 2.1.4: 2010/12/07

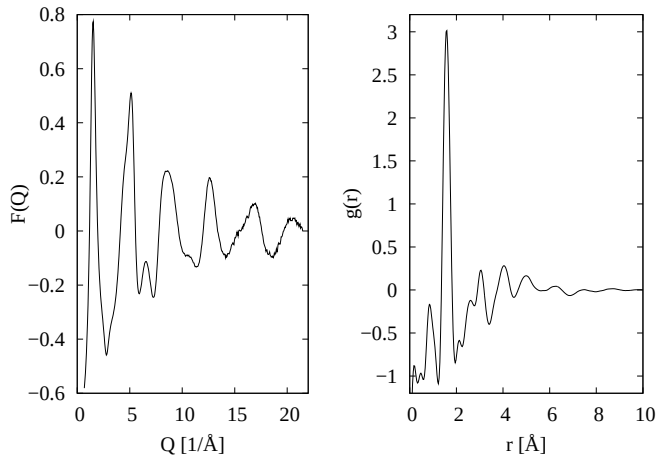

Figure 9
The structure function, $F(Q)$ (left), and corresponding PDF, $g(r)$, extracted using GudrunX for a solid amorphous silica rod of diameter 3mm, using Ag K_α radiation on a PANalytical x-ray diffractometer. The diffraction data were normalised to $\left(\sum_\alpha c_\alpha f_\alpha(Q)\right)^2$, and a top hat convolution width $Q_T = 2\text{Å}^{-1}$ and $r_{min} = 0.8\text{Å}$ were employed. The $g(r)$ were broadened by the method described in Appendix A, with $\Delta_0 = 0.12\text{Å}$ and $\beta = 0.2$ in (65).

6. Summary and Conclusions

The foregoing account has described in broad terms the functionality of a suite of programs design to reduce raw total x-ray scattering data to differential scattering cross section, and from there, via Fourier transform, to the pair distribution function. The method can process typical x-ray diffraction (XRD) data promptly and enough versality has been built into the code to allow a variety of materials to be processed, including those with significant fluorescent x-ray production. Standard corrections for attenuation, multiple scattering and background scattering are made, and a number of other x-ray specific corrections are available, including corrections for polarisation, Compton scattering, sample fluorescence, and bremsstrahlung radiation scattering. All these corrections are combined in the whole package, and the solution for the structure factor is achieved via an iterative process that calculates successive improvements to the final structure until a solution is found which is consistent with the required degree of Compton and bremsstrahlung scattering and fluorescence. Our experience to date is that although the user in principle has some choice over the various aspects of these corrections, such as the degree of bremsstrahlung scattering, f_{br}, or the x-ray fluorescence weights, w_e, and energies, $E_f^{(e)}$, in practice it is found that unless the choice is within a narrow range of values a satisfactory value of the structure factor is not obtained. Figure 4 shows the effect of not including a bremsstrahlung correction for example: if a bremsstrahlung factor of 0.4 had been used instead of 0.5, the resulting structure factor would have been notably worse.

It is quite likely that further improvements to the code can be envisaged, for example the automatic search of the above parameters to find the best possible solution, so that the user does not have to worry about those values. This might slow the code down a little, but make the outcome even more reliable. Equally other data formats could be envisaged, as could a more advanced fluorescence calculation for those materials where x-ray fluorescence is a serious problem. Yet another possibility is the idea that the atom form factors could be adjusted, perhaps with the assistance of neutron scattering data on the same material, to give the correct behaviour in $g(r)$ at low r. Much of the future development will depend on which features users of the software deem to be important.

Appendix A
A revised Lorch function

In his famous paper (Lorch, 1969), E. Lorch attempted to derive a function which would suppress the traditional truncation oscillations that bedevil direct Fourier transform of diffraction data. The success of his approach is marked by the almost universal adoption of his truncation function, $\dfrac{\sin Q\Delta}{Q\Delta}$, which goes to zero at and above $Q = Q_{max}$, and where $\Delta = \dfrac{\pi}{Q_{max}}$. (Note an unnecessary factor of 2 in the definition of Δ has been dropped here compared to Lorch's original definition.) The derivation of this function, however, contains an obvious flaw which can be shown simply by performing the integral that he claimed to have performed. The equation concerned is not numbered, but it occurs in section 3 of that paper, so it is quoted below:

$$\int_{r-\Delta}^{r+\Delta} 4\pi\, r^2\{h(r)\}\, dr = \frac{2}{\pi}\int_{r-\Delta}^{r+\Delta}\int_0^{Q_{max}} Qi(Q)\sin Qr\, dQ\, rdr \tag{58}$$

The idea here was to form the *average* of $h(r)$ over the region $r \pm \Delta$. Performing the r integral in (58) directly as instructed, we obtain:

$$\begin{aligned}\frac{1}{2\Delta}\int_{r-\Delta}^{r+\Delta} Q\sin Qr\, rdr &= \frac{1}{2Q\Delta}\Big[\sin Qr - Qr\cos Qr\Big]_{r-\Delta}^{r+\Delta} \\ &= \cos Qr\left(\frac{\sin Q\Delta}{Q\Delta} - \cos Q\Delta\right) \\ &\quad + Qr\sin Qr\frac{\sin Q\Delta}{Q\Delta}\end{aligned} \tag{59}$$

from which it can be seen that the Lorch function is only retrieved when $Q\Delta \ll \pi/2$, but this condition cannot be satisfied at $Q = Q_{max}$ by definition! Moreover this function certainly does not go to zero in that limit. So the function that has been used by researchers all over the world for more than 40 years to perform Fourier transforms of diffraction data was apparently based on faulty mathematics!

Notice the similarity between eq. (59) and the Fourier transform of the top hat function in section 5, eq. (51). This suggests a simple revision to the Lorch function, in keeping with his original vision of averaging $g(r)$ over a region of space. In effect

IUCr macros version 2.1.4: 2010/12/07

we will instead *smear* $g(r)$ uniformly over the region $|\mathbf{r} \pm \mathbf{\Delta}|$ by performing the same convolution of the top hat function as previously in Q-space, but now in r-space. Writing

$$\begin{aligned} L'(\mathbf{r}, \mathbf{\Delta}) &= \frac{3}{4\pi\Delta^3}, \quad |\mathbf{r}| \leq \Delta \\ &= 0, \qquad |\mathbf{r}| > \Delta \end{aligned} \tag{60}$$

the convolution of the radial distribution function with the top hat function is

$$\langle h(\mathbf{r}) \rangle_\Delta = \int_\Delta L'(\mathbf{r} - \mathbf{r}', \mathbf{\Delta})\, h(\mathbf{r}')\, d\mathbf{r}'. \tag{61}$$

Introducing the Fourier transform

$$h(\mathbf{r}) = \frac{1}{(2\pi)^3 \boldsymbol{\rho}} \int_{\mathbf{Q}} h(\mathbf{Q}) \exp[i\mathbf{Q} \cdot \mathbf{r}]\, d\mathbf{Q} \tag{62}$$

and the independent variable $\mathbf{r}'' = \mathbf{r} - \mathbf{r}'$ then

$$\begin{aligned} \langle h(\mathbf{r}) \rangle_\Delta &= \frac{1}{(2\pi)^3 \rho} \int_{\mathbf{Q}} \int_\Delta L'(\mathbf{r}'', \mathbf{\Delta}) \exp[-i\mathbf{Q} \cdot \mathbf{r}'']\, d\mathbf{r}'' \\ &\qquad \times h(\mathbf{Q}) \exp[i\mathbf{Q} \cdot \mathbf{r}]\, d\mathbf{Q} \\ &= \frac{1}{(2\pi)^3 \rho} \int_{\mathbf{Q}} L'(|\mathbf{Q}|, \Delta)\, h(\mathbf{Q}) \exp[i\mathbf{Q} \cdot \mathbf{r}]\, d\mathbf{Q}. \end{aligned} \tag{63}$$

where

$$L'(Q, \Delta) = \frac{3}{(Q\Delta)^3} (\sin Q\Delta - Q\Delta \cos Q\Delta). \tag{64}$$

Hence $L'(Q, \Delta)$ is the modified Lorch function, but note that it does not go to zero at $Q = Q_{max}$. In fact the form (64) suggests there is nothing to stop Δ being a width specified by the user, and moreover that width could in principle be a function of r, i.e. $\Delta = \Delta(r)$. In GudrunX a form for this variation is allowed:

$$\Delta(r) = \Delta_0 \left(1 + r^\beta\right) \tag{65}$$

with Δ_0 and β specified by the user, so the degree of broadening in r-space can vary with distance.

Appendix B
Towards accurate Fourier transforms

One final note concerns the evaluation of the integral (62). Normally $h(Q)$ is measured at discrete values of Q with each representing the average value of $h(Q)$ for each measurement bin. Hence the exact integral is normally replaced by a sum over values:

$$h(r) = \frac{1}{2\pi^2 \rho r} \sum_{Q_{min}}^{Q_{max}} h(Q) Q \sin Qr\; 2\Delta_Q(Q) \tag{66}$$

where $2\Delta_Q(Q)$ is the width of the bins which may in general be a function of Q. Comparing this with (62), and in keeping with the spirit of Lorch, it would make sense to average the function $Q \sin Qr$ over the bin width, i.e. instead of (66) we perform the average

$$\begin{aligned} h(r) &= \frac{1}{2\pi^2 \rho r} \sum_{Q_{min}}^{Q_{max}} h(Q) \int_{Q-\Delta_Q}^{Q+\Delta_Q} Q \sin Qr\; dQ \\ &= \frac{1}{2\pi^2 \rho r} \sum_{Q_{min}}^{Q_{max}} Q h(Q) \left[\cos Qr \left(\frac{\sin \Delta_Q r}{\Delta_Q r} - \cos \Delta_Q r \right) \right. \\ &\qquad \left. + Qr \sin Qr \frac{\sin \Delta_Q r}{\Delta_Q r} \right] 2\Delta_Q \end{aligned} \tag{67}$$

This reverts back to (66) in the event $\Delta_Q \to 0$. This expression is particularly useful when the Q bins are wide or vary in width with Q.

The authors are indebted to Daniel Bowron, Alex Hannon, David Keen and Matt Tucker for much advice on the contents of this paper and for a critical reading of the manuscript. David Keen and Antonio Cervellino are also to be thanked for supplying the synchrotron x-ray data used in testing the routines. In addition, the staff at PANalytical are to be thanked for ensuring the ISIS Disordered Materials x-ray diffractometer operated to the required specification, which enabled the work described here to be completed satisfactorily.

References

Balyuzi, H. H. M. (1975). *Acta. Cryst. Sect. A*, **31**, 600–602.
Billinge, S. J. L. & Thorpe, M. F. (eds.) (1998). *Local Structure from Diffraction*. Plenum Press, New York.
Blech, I. A. & Averbach, B. L. (1965). *Phys. Rev.* **137**, 1113–1116.
Breit, G. (1926). *Phys. Rev.* **27**, 362–372.
Compton, A. H. (1923). *Phys. Rev.* **21**, 483–502.
Dirac, P. (1926). *Proc. Roy. Soc. Lon. Series A*, **111**, 405–423.
Egami, T. & Billinge, S. J. L. (2003). *Underneath the Bragg Peaks: Structural Analysis of Complex Materials*. Pergamon/Elsevier, Oxford.
Faber, T. E. & Ziman, J. M. (1965). *Phil. Mag.* **11**(109), 153–&.
Hubbell, J. H. (1969). *Photon Cross Sections, Attenuation Coefficients and Energy Absorption Coefficients from 10 keV to 100 GeV*. Report NSRDS-NBS No. 29. Washington. DC: US Government Printing Office.
Hubbell, J. H. (1975). *J. Phys. Chem. Ref. Data*, **4**, 471 – 538.
Hubbell, J. H. (1977*a*). *J. Phys. Chem. Ref. Data*, **6**, 615 – 616.
Hubbell, J. H. (1977*b*). *Rad. Res.* **70**, 58 – 81.
Hubbell, J. H., Gimm, H. A. & Overbo, I. (1980). *J. Phys. Chem. Ref. Data*, **9**, 1023 – 1147.
Hubbell, J. H. & Overbo, I. (1979). *J. Phys. Chem. Ref. Data*, **8**, 69 – 105.
Hubbell, J. H., Veigele, W. J., Briggs, E. A., Brown, R. T., Cromer, D. T. & Howerton, R. J. (1975). *J. Phys. Chem. Ref. Data*, **4**, 471–538.
Jeong, I.-K., Thompson, J., Proffen, T., Turnera, A. M. P. & Billinge, S. J. L. (2001). *J. Appl. Cryst.* **34**, 536.
Kahn, R., Fourme, R., Gadet, A., Janin, J., Dumas, C. & Andre, D. (1982). *J. Appl. Cryst.* **15**, 330–337.
Kendig, A. P. & Pings, C. J. (1965). *J. of Appl. Phys.* **36**(5), 1692–1698.
Klein, O. & Nishina, Y. (1929). *Z. Phys.* **52**, 853–868.
Klug, H. P. & Alexander, L. E. (1954). *X-ray Diffraction Procedures: For Polycrystalline and Amorphous Materials*. Wiley, New York, 1st ed.
Krogh-Moe, J. (1956). *Acta Cryst.* **9**, 951–953.
Lorch, E. (1969). *J. Phys. C Solid State Phys.* **2**, 229–237.
McCall, G. H. (1982). *J. Phys. D Appl. Phys.* **15**, 823–831.

Norman, N. (1957). *Acta Cryst.* **10**, 370–373.
Paalman, H. H. & Pings, C. J. (1962). *J. Appl. Phys.* **33**, 2635–2639.
Petkov, V. (1989). *J. Appl. Cryst.* **22**, 387–389.
Pratt, R. H. (1960). *Phys. Rev.* **117**, 1017 – 1028.
Read, J. & Lauritsen, C. C. (1934). *Phys. Rev.* **45**(7), 433 – 436.
Ribberfors, R. (1983). *Phys. Rev. A*, **27**, 3061–3070.
Saloman, E. B. & Hubbell, J. H. (1986). *X-ray Attenuation Coefficients (Total Cross Sections): Comparison of the Experimental Data Base with Recommended Values of Henke and the Theoretical Values of Scofield for Energies between 0.1-100 keV*. Report NBSIR 86-3431. National Institute of Standards and Technology, Washington.
Saloman, E. B. & Hubbell, J. H. (1987). *Nucl. Inst. Meth. Phys. Res. Sec. A - Accelerators Spectrometers Detectors and Associated Equipment*, **255**, 38 – 42.
Scofield, J. H. (1973). *Theoretical Photoionization Cross Sections from 1 to 1500 keV*. Report UCRL-51326. Lawrence Livermore National Laboratory, California.
Soper, A. K. (1983). *Nucl. Inst. Meth. in Phys. Res.* **212**, 337–347.
Soper, A. K. (2007). *J. Phys. Condens. Matter*, **19**, 335206.
Soper, A. K. (2009). *Mol. Phys.* **107**, 1667–1684.
Soper, A. K. & Egelstaff, P. A. (1980). *Nucl. Inst. Meth.* **178**, 415–425.
Tucker, M. G., Keen, D. A., Dove, M. T., Goodwin, A. L. & Hui, Q. (2007). *J. Phys. Condens. Matter*, **19**, Art. 335218, 1–16.
Vineyard, G. H. (1954). *Phys. Rev.* **96**(1), 93–98.
Waasmaier, D. & Kirfel, A. (1995). *Acta. Cryst.* A**51**, 416–431.
Warren, B. E. (1968). *X-ray Diffraction*. Reading: Addison-Wesley, U.S.